CORROSION SCIENCE AND TECHNOLOGY, Vol.24, No.1(2025), pp.1~10
[Research Paper]
pISSN 1598-6462 / eISSN 2288-6524
DOI: https://doi.org/10.14773/cst.2025.24.1.1

Comparative Study of Corrosion Behavior of AA6061 and AA5086 Aluminum Alloys in Polluted Local Seawater -Iraq

Mohanad Muzahem Khalaf [1], Al-Ezzi Salih[1], Taha H. Abood Al-Saadi[1], and A. M. Mustafa[2,†]

[1]*Materials Techniques Engineering Department, Technical Engineering College-Baghdad, Middle Technical University, Iraq*
[2]*Production Engineering and Metallurgy Department, University of technology, Baghdad, Iraq*
(Received August 13, 2024; Revised October 14, 2024; Accepted October 14, 2024)

This study investigated the electrochemical corrosion performance of AA6061 and AA5086 alloys in local seawater (LSW) at both low and high temperatures, reflective of conditions in the Iraqi environment. An electrochemical technique was employed to assess the corrosion behavior of the alloys in locally polluted seawater and a 3.5 wt% NaCl solution. The specimens were tested at various temperatures (5, 15, 25, 35, 45, and 55 °C) and compared to a 3.5 wt% NaCl solution at room temperature. Optical, microscopic, and SEM tests were conducted on the corroded surfaces. The results revealed that the corrosion rate increased with temperature, and there was a noticeable increase in the depth and distribution of pitting as temperature rose. Generally, the pitting potential (Ep) values for AA5085 were higher than those for AA6061 alloys. Although the corrosion current densities for AA5086 and AA6061 in the NaCl solution were similar (0.26 and 0.2 mA/cm^2, respectively), AA6061 exhibited a six-fold lower electrochemical corrosion current density compared to AA5086 at 25 °C in locally polluted seawater (LSW).

Keywords: *Local Seawater (LSW), AA5086, AA6061, Electrochemical corrosion*

1. Introduction

Aluminum alloys are extensively used in aerospace, automotive, and marine applications [1,2]. While the lack of rainfall and the effect of seawater intrusion into the Shatt al-Arab changed the chemical properties [3], The Middle East has recorded the highest temperature in the world many times in the last few years. Different types of aluminum alloys are connected, riveted [4], welded [5,6], and clenched by manufacturing processes. While these alloys form a protective passive oxide film (Al_2O_3) on their surfaces, they present good corrosion resistance in many environments with a neutral pH, owing to the insoluble oxide film in water [7]. However, the concentration of specific sea pollutants and microorganisms can accelerate or mitigate the corrosion of metals [8-10]. M. Teyaka [11] investigated the corrosion behavior of three types of aluminum welded alloys using shielded metal arc welding, friction stir welding, and gas tungsten arc welding. The results revealed that the samples of friction stir welding showed better corrosion resistance than those of the other welding processes. NR Ramesh *et al.* [12] studied the erosion-corrosion response of AA5083 and AA6061 welded joints for various combinations of pH values due to the change of pH in seawater during the monsoon and post-monsoon seasons.

Their results approved that the pH has the most predominant parameter on the erosion-corrosion behavior of the combination of the welded joint, up to 86.89%. On the other side, the investigation of the corrosion behavior of the aluminum alloys was carried out separately. An investigation was conducted to study the impact of heat treatment parameters on the corrosion behavior of aluminum alloys AA6061, AA6013, and AA5086 [13]. They noticed that the corrosion resistance decreased for quenched samples at 530 °C in comparison to artificial and natural-aged samples. Temperature has a direct impact on the corrosion rate and corrosion behavior of materials, as well as the activity of corrosion inhibitors [14]. It was noticed that the inhibition efficiency of chloramphenicol decreased with the increase in temperature from 30 °C to 60 °C [15]. The study by Samar S. *et al.* showed that the rate of corrosion for Ni-Cr alloy goes up noticeably as the temperature rises (30 °C to 60 °C), but copper showed

†Corresponding author: Ali.M.Mustafa@uotechnology.edu.iq

clear corrosion resistance at most of the temperatures that were looked at. Also, the N.O. Obi-Egbedi *et al.* [16] investigation revealed that the xanthene's inhibition efficiency of mild steel corrosion rate was found to increase with concentration increasing but decreased with temperature increasing to 60 ºC. In addition, Chen Xin *et al.* [14] found that the corrosion current and the cathodic reaction rate of the 3003-aluminum alloy rose dramatically to their maximum at 60 ºC. Finally, the researchers [17-19] investigated the corrosive environments and inhibitory of metals at low and high temperatures. However, the effect of the local water pollution during the lack of rainfall and oil production in the south of Iraq still needs deep investigation for the corrosion of aluminum and other metals [20-22].

This study aims to determine whether the locally polluted seawater and temperature are inhibiting or accelerating the corrosion behavior of AA6061 and AA5086 aluminum alloys. The selected the polluted seawater from a location that has consistently recorded the highest global temperatures in recent years. In addition, according to previous research [23-26], the 5xxx alloys can experience intergranular corrosion (IGC) if the electrochemically active β'phase (Al_3Mg_2) precipitates form at the grain boundaries. So, it is worth investigating this alloy's behavior in LSW environments and comparing the results to the corrosion in saline solution [27,28].

2. Materials and Experimental Methods

In this study, AA6061 and 5086 aluminum alloy plates were used. Table 1 presents the elemental composition of the aluminum alloys studied using spark analysis. The aluminum samples were prepared with dimensions of 20 × 20 × 8 mm. Square-shaped aluminum alloy specimens, exposed to a surface area of 0.785 cm^2, served as the electrodes for the polarization measurement. We ground it using different grades of grinding papers (400, 800, and 1200 grit) and then polished it with diamond paste. Then, samples were degreased with ethanol, rinsed with distilled water, and finally dried to prepare for use in the brine solutions. In this work, two types of environments were used: local seawater (LSW) from the south of Iraq (Basrah-end point of Shat Al-Arab), and a brine solution containing 3.5 wt% NaCl. Table 1 illustrates the chemical composition of local seawater. Table 2 illustrates the elemental compositions of the studied alloys with total dissolved solids (TDS) and electrical conductivity (Ec).

By using an electrochemical technique, the examination was carried out in stagnant open-air conditions in a 500-ml volume cell using a thermostat-controlled water bath, and the experiments were conducted at different temperatures (5, 15, 25, 35, 45, and 55 ºC). A graphite sheet was used (7 cm^2 area) as a counter electrode in the conventional three-electrode cell system, employing silver-silver chloride (Ag/AgCl) as a reference electrode. It is connected with an aluminium alloy sample as a

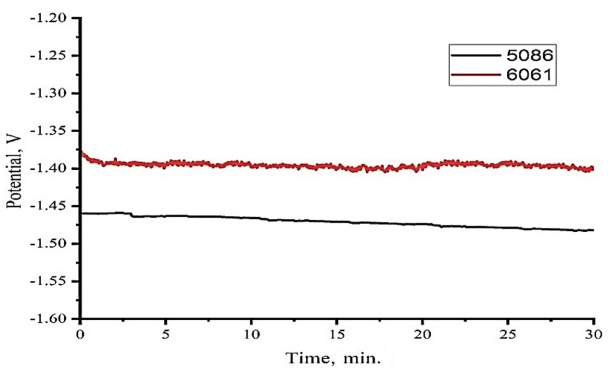

Fig. 1. OCP of AA6061 and AA5086 alloys in 3.5% NaCl at 25 ºC

Table 1. Elemental composition of AA6061 and AA5086 alloys

Elements (wt%)	Mg	Si	Fe	Cu	Cr	Mn	Ti	Zn	V	Al
AA6061	1.3	0.7	0.52	0.28	0.21	0.15	0.08	0.05	0.04	96.94
AA5086	3.5	-	0.5	0.1	0.25	0.7	-	-	-	94.95

Table 2. Chemical composition of local seawater (LSW)

Local Sea Water	TDS (mg/L)	Ec (S/cm)	Na (mg/L)	Cl (mg/L)	Ca (mg/L)	Mg (mg/L)	SO_4 (mg/L)	HCO_3 (mg/L)	CO_3 (mg/L)	pH
	36838	0.709	14700	3840	8000	1940	757.5	70	40	8.5

working electrode. The performe of the potentiodynamic polarization experiment at a scan rate of 0.01 V/s. The conducted this investigation using the DY2321 Potentiostat station. Fig. 1 illustrates the open circuit potential (E_{ocp}) of the studied alloys in a brine solution (3.5 wt% NaCl) at 30 min. The calculated the corrosion current density ($I_{corr.}$) and corrosion potential ($E_{corr.}$) using a Tafel-type fit from the polarization curves.

3. Results and Discussion

3.1 Corrosion behavior at room temperature

Fig. 2 illustrates the corrosion behavior of AA5086 and AA6061 alloys. They were tested in local seawater (LSW) and 3.5 wt% NaCl at room temperature. The evaluation showed that the alloys behaved similarly in saline solutions. The results show the pitting potential ($E_{p.}$) values of -0.813, -0.71 V, and -0.635, -0.485 V for AA6061 and AA5086 alloys at 3.5 wt% NaCl solution and LSW, respectively. It can be concluded that the sample AA5086 possesses a better resistance to pitting corrosion as compared with AA6061 in the studied environments.

3.2 Corrosion behavior at various temperatures

The polarization curves for AA6061 and AA5086 aluminum alloys in local seawater (LSW) at varying temperatures provide valuable insights into the corrosion behavior of these materials under different thermal conditions. temperature is a critical factor influencing the corrosion behavior of aluminum alloys. As the temperature increases, the corrosion rate typically increases due to the enhanced electrochemical activity and the accelerated kinetics of corrosion reactions. Figs. 3a and b illustrate the polarization curves for two aluminum alloys studied (i.e., AA6061 Fig. 3a and AA5086 Fig. 3b) in local seawater (LSW) at temperatures ranging from 5 to 55 ºC.

Table 3 illustrates all the results (corrosion rate, $E_{corr.}$, $I_{corr.}$, and $E_{p.}$) recorded from the electrochemical technique for the studied alloys (i.e., AA5086 and AA6061). For

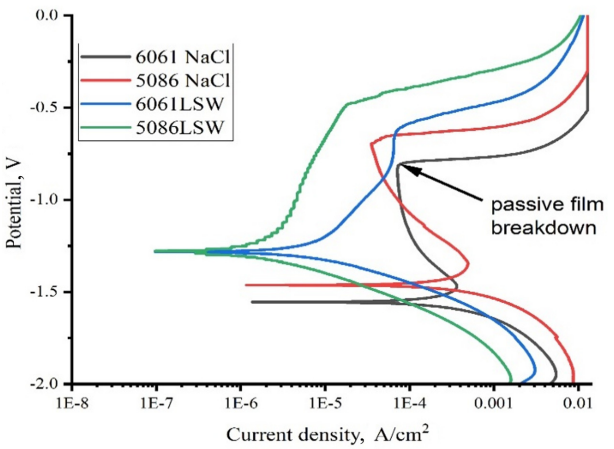

Fig. 2. The polarization curves for AA6061 and AA5086 alloys in 3.5 wt% NaCl and LSW at 25 ºC

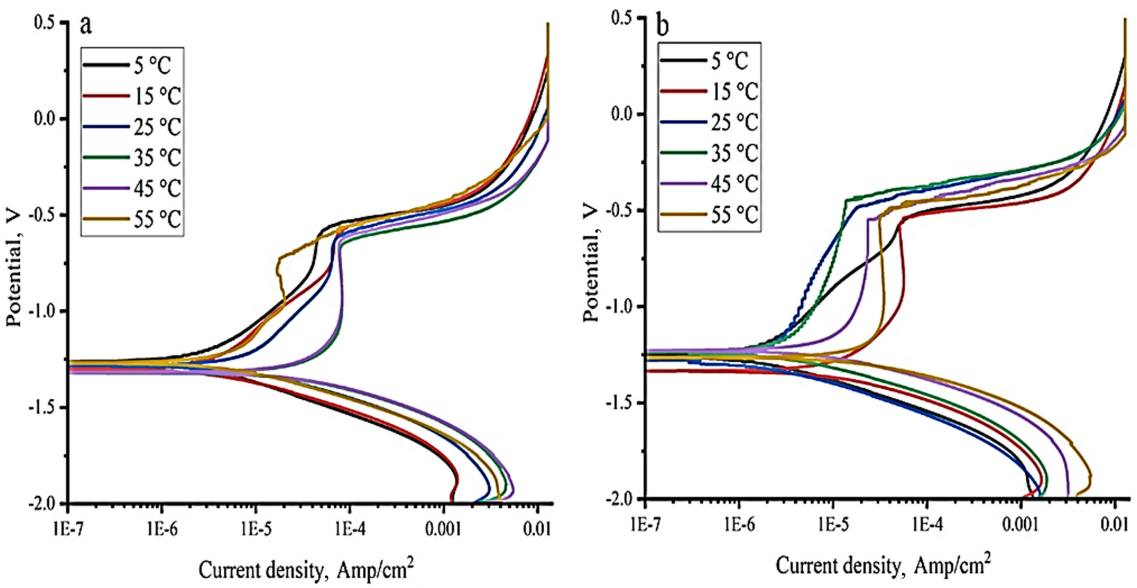

Fig. 3. The polarization curves of a) AA6061 and b) AA5086 alloys at various temperatures 5 to 55 ºC in LSW

AA5086, the corrosion rate increases with the increase or decrease in temperature in comparison to 25 ºC, while for AA6061, the corrosion rate increases with the increase in temperature to 45 ºC. On the other hand, the recorded $E_{p.}$ is slightly varying (-0.452 to -0.59 V) for AA5086 with the variation of LSW temperature. While for AA6061, $E_{p.}$ is widely varying (-0.445 to 0.725 V) with the variation of LSW temperature.

The recorded result (Table 3) shows that, the $I_{corr.}$ values increase with temperatures rising from 5 to 45 ºC. This is due to the direct effect of temperature on the oxide layer formed on the AA6061 alloy's surface. While the $I_{corr.}$ value decrease at 55 ºC, this is most probably due to the passivity phenomena of this alloy at high temperature. For AA5086 Al alloy, the variation in $I_{corr.}$ values were noticed, depending on the alloy's behavior when exposed to different temperatures from (5 to 55 ºC), with using the same environment. This is due to the corrosion resistance ability of this alloy by forming an oxide layer. In the 3.5 wt% NaCl solution at room temperature, the Ep for AA6061 is less than AA5086, according to Fig. 4. Finally, it can be concluded that the AA5086 is more resistant than the AA6061in a selective environment.

From Fig. 4, the pitting potential value ($E_{p.}$) for AA5086 increases (less Increased temperatures (from 5, 15, 25, 35, and 45 ºC) result in the formation of an oxide film, which protects the alloy from the environment. While a decrease in the $E_{p.}$ (more negative direction) value at a temperature of 55 ºC due to the direct effect of high temperature on the oxide film formation on the alloy surface.

On the contrary, for AA6061, the Ep value decreases (with more negative values) with increasing temperatures from 5 to 55 ºC, except at 45 ºC. This is because the oxide film of this alloy does not resist the solution's rising temperatures. Also, it can be observed that at a temperature of 45 ºC, the alloy counteracts the aggressiveness of the solution (i.e., the value increases).

Table 3. The corrosion rate, $E_{corr.}$, $I_{corr.}$ and $E_{p.}$ For AA5086 and AA6061 at various temperatures from (5 to 55 °C) in LSW

Temp. (°C)	corrosion rate (mm/year)		$E_{corr.}$(V)		$I_{corr.}$ (µA/cm²)		$E_{p.}$ (V)	
	AA5086	AA6061	AA5086	AA6061	AA5086	AA6061	AA5086	AA6061
5	1.05E-02	1.60E-02	-1.257	-1.265	0.758	1.16	-0.59	-0.61
15	7.08E-02	2.28E-02	-1.335	-1.298	5.11	1.65	-0.575	-0.625
25	7.98E-03	4.93E-02	-1.279	-1.284	0.576	3.55	-0.485	-0.658
35	1.63E-02	1.88E-01	-1.235	-1.321	1.17	13.6	-0.452	-0.665
45	5.63E-02	1.86E-01	-1.228	-1.318	4.06	13.4	-0.456	-0.445
55	1.35E-01	3.26E-02	-1.265	-1.267	9.71	2.35	-0.51	-0.725

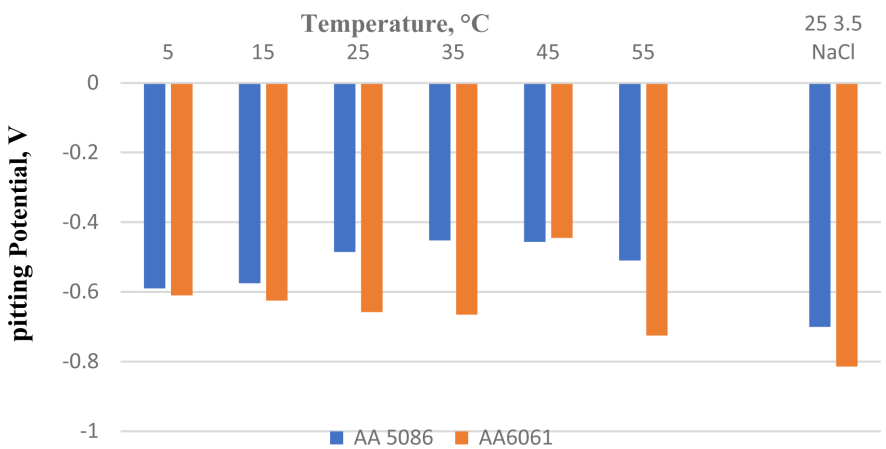

Fig. 4. The pitting potential ($E_{p.}$) of AA6061 and AA5086 at various temperatures (5 to 55 °C) in LSW solution and 3.5 wt% of NaCl solution at 25 °C.

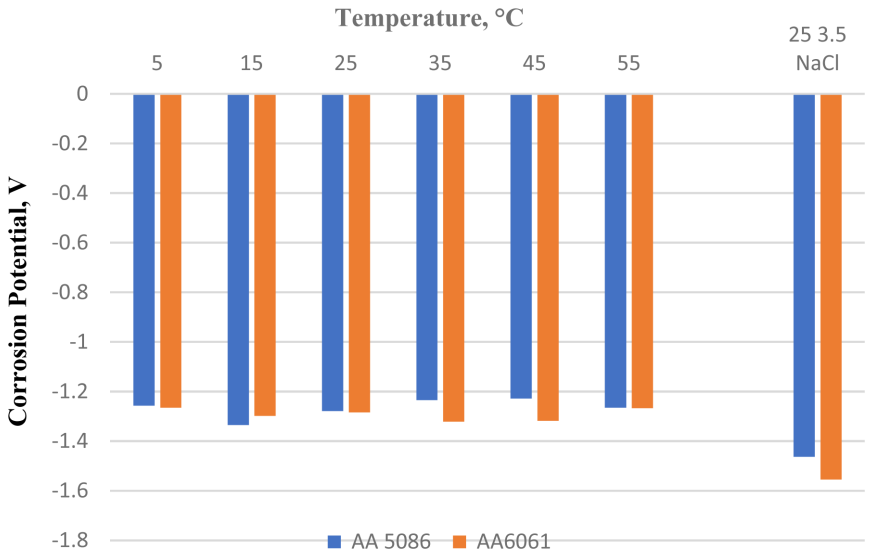

Fig. 5. The corrosion potential ($E_{corr.}$) of AA6061 and AA5086 at various temperatures from (5 to 55) °C in LSW solution and 3.5 wt% of NaCl solution at 25 °C

Fig. 5 illustrates the influence of various temperatures and solutions on the corrosion potential of two studied alloys. It can be seen that there is no direct effect of the increasing temperature from 5 to 55 °C on the $E_{corr.}$ for AA5086 and AA6061 at LSW solution (i.e., extremely constant). While a decrease in the $E_{corr.}$ value for AA5086 and AA6061 in 3.5 wt% of NaCl solution at room temperature as compared with LSW solution (i.e., aggressive solution). The corrosion behavior of Al alloys (AA6061 and AA5086) is associated with chlorine adsorption on the initiated passive film and film breakdown [20]. However, the difference in corrosion behaviors for the aluminum alloys in LSW and 3.5 wt% NaCl was a hindrance to the investigation of the LSW effect at different temperatures.

Fig. 6 illustrates the corrosion rate (mm/year) for the two studied alloys at different temperatures and solutions. From results, low corrosion rate values for the two studied alloys were recorded (i.e., a slight increase with increasing

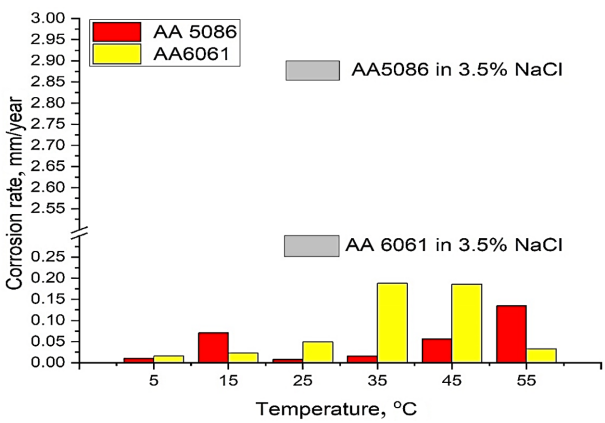

Fig. 6. The corrosion rate of AA6061 and AA5086 at various temperatures from (5 to 55) °C in LSW solution and 3.5 wt% of NaCl solution at 25 °C

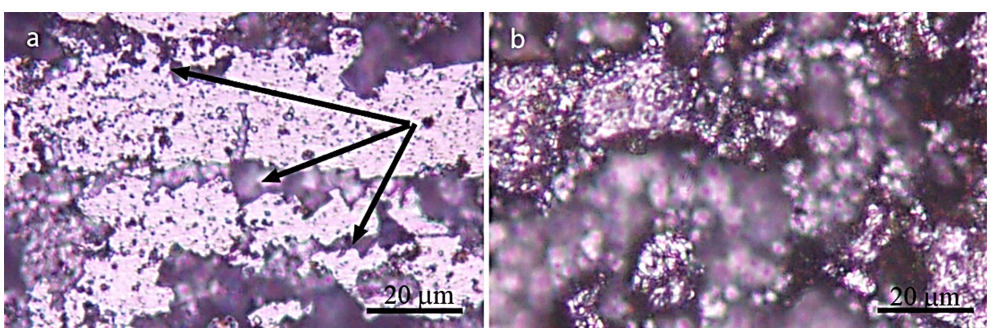

Fig. 7. Corrosion of alloys in 3.5%NaCl a) Intergranular corrosion (IGC) formation at the grain boundary of AA5086, b) deep pitting on the surface of AA6061

temperatures from 5 to 55 °C). This is due to the tendency of these alloys to create an oxide film on the surface (passivity behavior) in the LSW solution. However, there is a sharp increase in corrosion rate values for AA6061

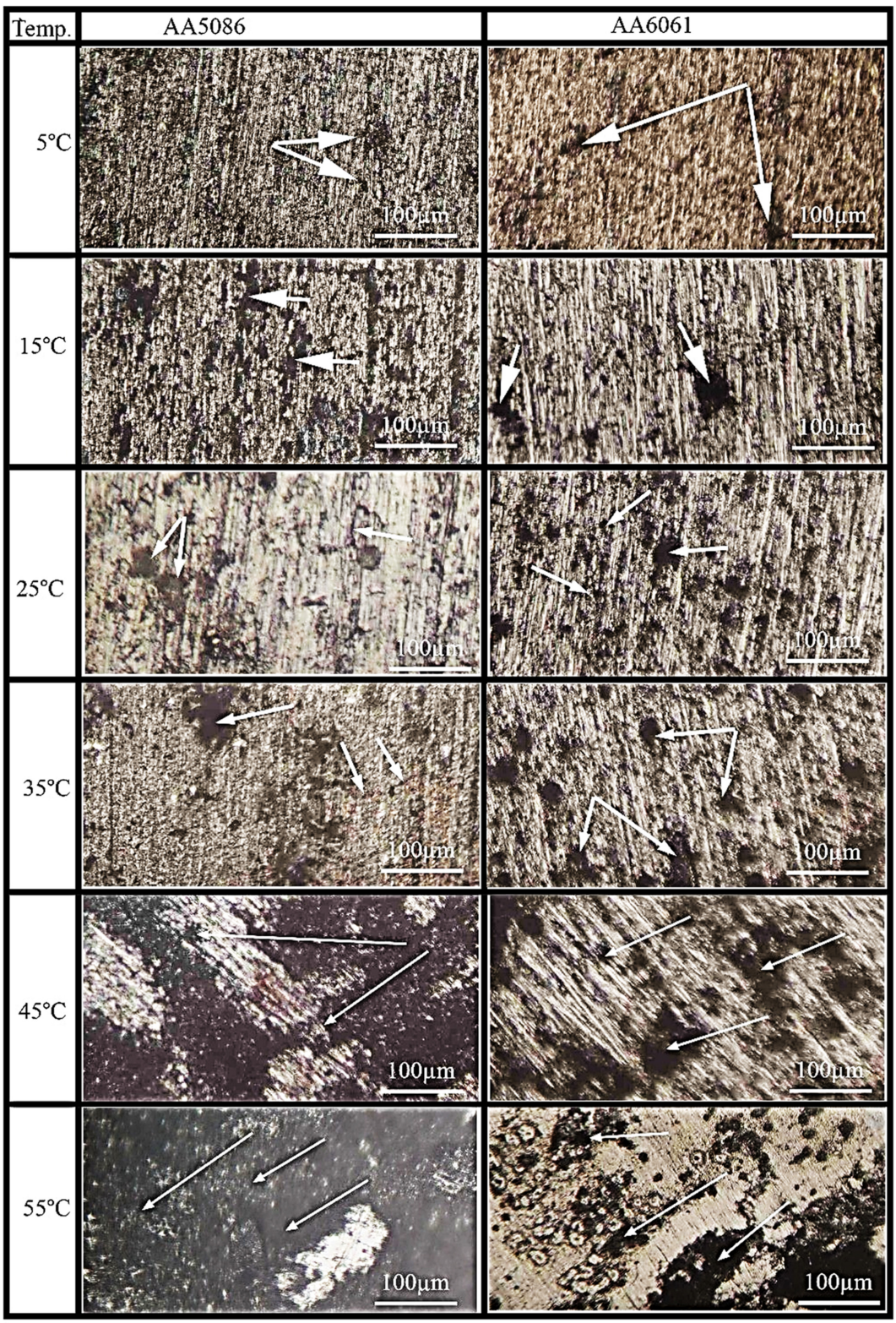

Fig. 8. Microstructure images of AA6061 and AA5086 at various temperatures from 5 to 55 °C in LSW

as compared with AA5086. This is due to the aggressive solution of brine solution (3.5 wt% NaCl), which can penetrate and break the oxide layer initiated on the alloy surface, thus accelerating the corrosion of the alloy. On the other side, the presence of Fe has a high percentage as compared with the AA5086 alloy.

It is worth mentioning that the high percentage of Cr in the AA5085 alloy (see Table 1) accelerates the formation of intermetallic compounds (IMC), which affect the bulk properties of the alloy.

This IMC results in high surface roughness. Fig. 7a shows the intergranular corrosion (IGC) formation at the grain boundary of AA5086 in 3.5% NaCl. This is due to the large size of IMC (Al_3Mg_2), resulting in high surface roughness, which may affect corrosion resistance [21]. While Fig. 7b illustrates deep corrosion in different locations of AA6061.

3.3 Microstructure Analysis

Fig. 8 presents the microstructure images of the studied aluminum alloys at different temperatures from 5 to 55 ºC in LSW, which were examined by an optical microscope. The surface of the investigated alloys displayed localized corrosion (pitting) of varying sizes, which intensified as the temperature increased, as indicated by the white arrows. The surface pitting on aluminum alloys occurs when an electrolyte is present, and it increases as the temperature rises because of the aggressive ion concentration and electrolyte stagnation [29]. Furthermore, according to Joule's law, as the temperature increases, the diffusion rate increases and, in conjunction with the decreases of electrolyte resistance, which accelerates the corrosion rate. It was recorded that the corrosion rate increased significantly with the increasing temperature [30].

3.4 SEM and EDS analysis

As you can see in Fig. 9, the AA5086 and AA6061 surfaces that were corroded in 3.5% NaCl and LSW solutions are shown using scanning electron microscopy (SEM). Figs. 9a and b illustrate the morphology of the corrosion products on the alloy surface in 3.5% NaCl. When comparing the surface of corrosion products formed on alloys in LSW, Figs. 9c and d show a different morphology due to the presence of many compounds

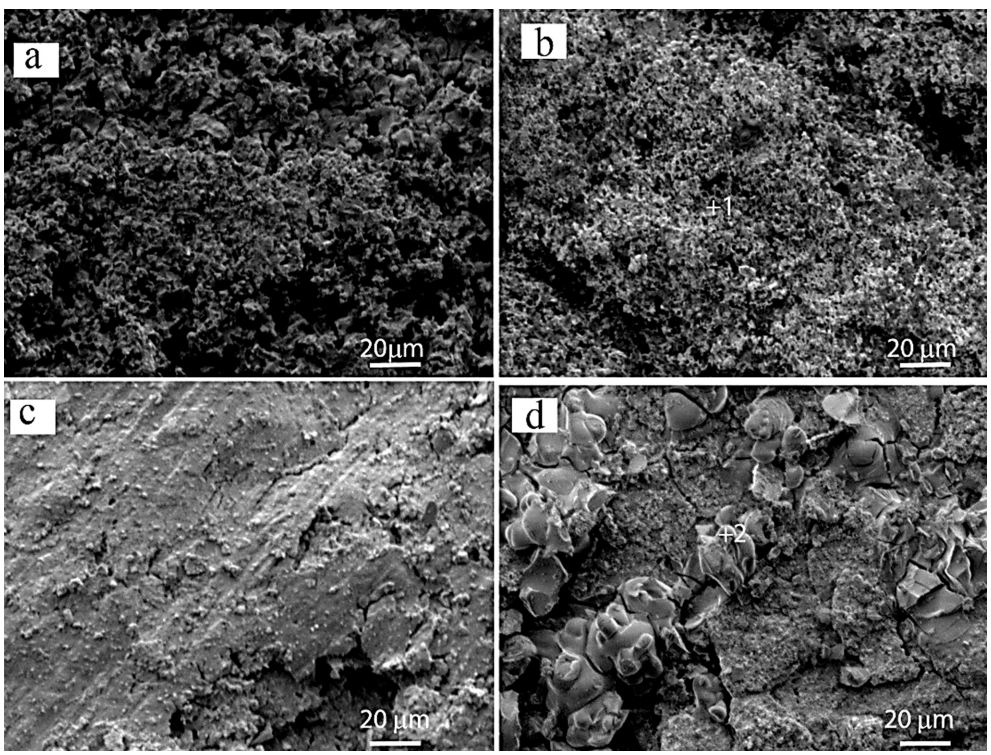

Fig. 9. SEM images for a) corroded surface of AA5086 in 3.5%NaCl, b) corroded surface of AA6061 in 3.5%NaCl, c) corroded surface of AA5086 in LSW, d) corroded surface of AA6061 in LSW

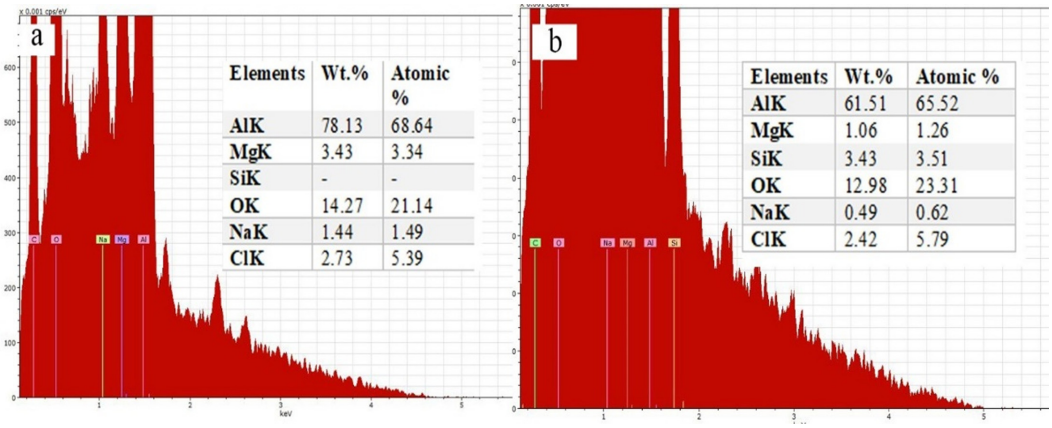

Fig. 10. EDS analysis of corrosion product in LSW for: a) AA5086 and b) AA6061

other than NaCl, as listed in Table 2. Fig. 10 presents the EDS of the two aluminum alloys under study. For AA5086, the main components are Al, Mg, and Na, while for AA6061, they are Al, Mg, Si, and Na. The decrease in Al and Mg contents could potentially result in the formation of various corrosion products on the surfaces. The roughness of samples is caused by Insufficient time at each polishing stage might leave deeper scratches from coarser grits and the grit was the max of grit is 1200. Also, corrosion residues on the surface may lead to surface roughness.

4. Conclusion

The effect of temperatures on the corrosion behavior of AA5086 and AA6061 aluminum alloys has been conducted by using two types of surrounding media (i.e., local sea water and 3.5 wt% NaCl solution). The corrosion rates (mm/y) increased with temperature. Moreover, the size and distribution of localized pits showed an obvious increment with the increase in temperature. Generally, the pitting potential ($E_{p.}$) values for AA5086 were higher than those for AA6061 alloys, and it can be concluded that the AA5086 alloy has resistance to localized (pitting) corrosion as compared with AA6061 due to the chemical composition content (i.e., Cr and Mn content).

References

1. I. H. Zainelabdeen, F. A. Al-Badour, R. K. Suleiman, A. Y. Adesina, N. Merah, and F. A. Ghaith, Influence of Friction Stir Surface Processing on the Corrosion Resistance of Al 6061, *Materials (Basel),* **15**, 8124(2022). Doi: https://doi.org/10.3390/ma15228124
2. H. Zhu, Z. Huang, G. Jin, and M. Gao, Effect of temperature on galvanic corrosion of Al 6061-SS 304 in nitric acid, *Energy Reports,* **8**, 112 (2022). Doi: https://doi.org/10.1016/j.egyr.2022.10.022
3. B. R. Yaseen, K. A. A. Asaady, A. A. Kazem, and M. T. Chaichan, Environmental Impacts of Salt Tide in Shatt Al-Arab-Basra/Iraq (2016). Doi: http://dx.doi.org/10.9790/2402-10123543
4. J. F. C. D. Moraes, H. Rao, and J. B. Jordon, *Proc. 23rd ABCM International Congress of Mechanical Engineering Conf.*, Elucidating The Effect of Contact Stresses in Dissimilar Aluminum-To-Aluminum Joining Via Self-Pierce Riveting (2015).
5. N. Wohner and L. H. Hihara, ECS MeetingCorrosion Morphologies in Different Welding Zones of Friction-Stir Welded (FSW) Aluminum Alloy AA5086AA5086, AA6061AA6061, and Dissimilar AA5086AA6061 Joints Exposed in Various Atmospheric Environments, *ESC Meeting Abstracts*, **MA2016-02**, 1123 (2016). Doi: https://doi.org/10.1149/MA2016-02/9/1123
6. S. K. Hussein, M. K. Abbass, and A. Baqer, Analysis of Fatigue in Friction Stir Welding Regions of AA5086-H32 to AA6061-T6 Aluminum Alloys, (2017). https://www.researchgate.net/publication/320237227_ANALYSIS_OF_FATIGUE_IN_FRICTION_STIR_WELDING_REGIONS_OF_AA5086-H32_TO_AA6061-T6_ALUMINUM_ALLOYS
7. G. Acosta, L. Veleva, J. L. LÓPez, and D. A. LÓPez-Sauri, Contrasting initial events of localized corrosion on surfaces of 2219-T42 and 6061-T6 aluminum alloys exposed in Caribbean seawater, *Transactions of Nonferrous Metals Society of China,* **29**, 34 (2019). Doi: https://

doi.org/10.1016/s1003-6326(18)64912-x

8. J. F. Marques, Benedandti, and C. J. Bioelectrochemistry, Influence of natural seawater variables on the corrosion behavior of aluminium-magnesium alloy, *Bioelectrochemistry*, **149**, 108321 (2023). Doi: https://doi.org/10.1016/j.bioelechem.2022.108321
9. Y. Cai, Y. Xu, Y. Zhao, W. Zhang, J. Yao, M. Wei, K. Zhou, X. Ma, Quantitative Understanding of the Environmental Effect on B10 Copper Alloy Corrosion in Seawater, *Metals*, **11**, 1080 (2021). Doi: https://doi.org/10.3390/met11071080
10. K. Wang, J. Jia, W. Chen, and N. J. T. I. He, Investigation of corrosion and wear properties of Si3N4-hBN ceramic composites in artificial seawater, *Tribology International*, **164**, 107235 (2021). Doi: https://doi.org/10.1016/j.triboint.2021.107235
11. M. Teyaka and H. A. J. I. J. o. E. Science, A study on the corrosion behavior in seawater of welds aluminum alloy by shielded metal arc welding, friction stir welding and gas tungsten arc welding, *International Journal of Electrochemical Science*, **10**, 8549 (2015). Doi: https://doi.org/10.1016/S1452-3981(23)11118-7
12. N. R. Ramesh and V. S. S. J. A. O. R. Kumar, Experimental erosion-corrosion analysis of friction stir welding of AA 5083 and AA 6061 for sub-sea applications, *Applied Ocean Research*, **98**, 102121 (2020). Doi: https://doi.org/10.1016/j.apor.2020.102121
13. E. F. A. Zeid, Mechanical and electrochemical characteristics of solutionized AA 6061, AA6013 and AA 5086 aluminum alloys, *Journal of Materials Research and Technology,* **8**, 1870 (2019). Doi: https://doi.org/10.1016/j.jmrt.2018.12.014
14. X. Chen, W. Tian, S. Li, M. Yu, and J. Liu, Effect of temperature on corrosion behavior of 3003 aluminum alloy in ethylene glycol–water solution, *Chinese Journal of Aeronautics,* **29**, 1142 (2016). Doi: https://doi.org/10.1016/j.cja.2015.12.017
15. B. M. Prasanna, B. M. Praveen, N. Hebbar, and T. V. Venkatesha, Corrosion inhibitory action of mild steel in 1M HCl by Chlorophenicol, *Moroccan Journal of Chemistry*, **4**, 824 (2015). Doi: https://doi.org/10.48317/IMIST.PRSM/morjchem-v3i4.3229
16. N. Obi-Egbedi and I. J. A. J. o. C. Obot, Adsorption behavior and corrosion inhibitive potential of xanthene on mild steel/sulphuric acid interface, *Arabian Journal of Chemistry*, **5**, 121 (2012). Doi: https://doi.org/10.1016/j.arabjc.2010.08.004
17. X. Cao *et al*., Corrosion behavior of aluminum alloy in sulfur-associated petrochemical equipment H2S environment, Chemical Engineering Communications, *Chemical Engineering Communications*, **210**, 233 (2023). Doi: https://doi.org/10.1080/00986445.2022.2030729
18. V. Konovalova, The effect of temperature on the corrosion rate of iron-carbon alloys, *Materials Today: Proceedings*, **38**, 1326 (2021). Doi: https://doi.org/10.1016/j.matpr.2020.08.094
19. A. R. Prabhukhot, Effect of Heat Treatment on Hardness and Corrosion Behavior of 6082-T6 Aluminium Alloy in Artificial Sea Water, *International Journal of Materials Science and Engineering*, **3**, 287 (2015). Doi: https://doi.org/10.17706/ijmse.2015.3.4.287-294
20. Y. Ji, Q. Hu, D.-H. Xia, and J.-L. Luo, Corrosion Susceptibility of Passive Films on 1060, 2024, and 5083 Aluminum Alloys: Experimental Study and First-Principles Calculations, *Journal of The Electrochemical Society*, **170**, 041505 (2023). Doi: https://doi.org/10.1149/1945-7111/accab8
21. P. Budsarakham, C. Riyaphan, R. Canyook, and K. Taweesup, Effects of Cr on anodizing and microstructure of cast aluminum alloys, *Materials Today: Proceedings*, **5**, 9417 (2018). Doi: https://doi.org/10.1016/j.matpr.2017.10.119
22. Firas F. Sayyid, Ali M. Mustafa, Slafa I. Ibrahim, Mustafa K. Mohsin, Mahdi M. Hanoon, Mohammed HH Al-Kaabi, A. A. H. Kadhum, Wan Nor Roslam Wan Isahak, and A. A. Al-Amiery, Gravimetric Measurements and Theoretical Calculations of 4-Aminoantipyrine Derivatives as Corrosion Inhibitors for Mild Steel in Hydrochloric Acid Solution: Comparative Studies, *Corrosion Science and Technology*, **22**, 73 (2023). Doi: https://doi.org/10.14773/cst.2023.22.2.73
23. A. M. Mustafa, Z. S. Abdullahe, F. F. Sayyid, M. M. Hanoon, A. A. Al-Amiery, and W. N. R. W. Isahak, 3-Nitrobenzaldehyde-4-phenylthiosemicarbazone as Active Corrosion Inhibitor for Mild Steel in a Hydrochloric Acid Environment, *Progress in Color, Colorants and Coatings*, **15**, 285 (2022). Doi: https://doi.org/10.30509/pccc.2021.166869.1127
24. Firas F. Sayyid, Ali M. Mustafa, Mahdi M. Hanoon, Lina M. Shaker, and Ahmed A. Alamiery, Corrosion Protection Effectiveness and Adsorption Performance of Schiff Base-Quinazoline on Mild Steel in HCl Environment, *Corrosion Science and Technology*, **21**, 77 (2022). Doi: https://doi.org/10.14773/cst.2022.21.2.77

25. M. K. Abbass, K. M. Raheef, I. A. Aziz, M. M. Hanoon, A. M. Mustafa, W. K. Al-Azzawi, A. A. Al-Amiery, and A. A. H. Kadhum, Evaluation of 2-Dimethylaminopropionamidoantipyrine as a Corrosion Inhibitor for Mild Steel in HCl Solution: A Combined Experimental and Theoretical Study, *Progress in Color, Colorants and Coatings*, **17**, 1 (2024).Doi: https://doi.org/10.30509/PCCC.2023.167134.1216
26. M. Taha Mohamed, S. A. Nawi, A. M. Mustafa, F. F. Sayyid, M. M. Hanoon, A. A. Al-Amiery, A. A. H. Kadhum, and W. K. Al-Azzawi, Revolutionizing Corrosion Defense: Unlocking the Power of Expired BCAA, *Progress in Color, Colorants and Coatings*, **17**, 97 (2024). Doi: https://doi.org/10.30509/pccc.2023.167156.1228
27. A. Y. I. Rubaye, M. T. Mohamed, M. A. I. Al-Hamid, A. M. Mustafa, F. F. Sayyid, M. M. Hanoon, A. H. Kadhum, A. A. Alamiery, and W. K. Al-Azzawi, Evaluating the corrosion inhibition efficiency of 5-(4-pyridyl)-3-mercapto-1, 2, 4-triazole for mild steel in HCl: insights from weight loss measurements and DFT calculations, *Intternational Journal of Corrosion and Scale Inhibition*, **13**, 185 (2024). Doi: https://doi.org/10.17675/2305-6894-2024-13-1-10
28. N. S. Abtan, A. E. Sultan, F. F. Sayyid, A. A. Alamiery, A. H. Jaaz, T. S. Gaaz, S. M. Ahmed, A. M. Mustafa, D. A. Ali and M. M. Hanoon, Enhancing corrosion resistance of mild steel in hydrochloric acid solution using 4-phenyl-1-(phenylsulfonyl)-3-thiosemicarbazide: A comprehensive study, *International Journal of Corrosion and Scale Inhibition*, **13**, 435 (2024). Doi: https://doi.org/10.17675/2305-6894-2024-13-1-22
29. Hosni Ezuber, A. El-Houd, F. El-Shawesh, A study on the corrosion behavior of aluminum alloys in seawater, *Materials & Design*, **29**, 801 (2008). Doi: https://doi.org/10.1016/j.matdes.2007.01.021
30. J. Soltis, N. J. Laycock, D. Krouse, Temperature dependence of the pitting potential of high purity aluminium in chloride containing solutions, *Corrosion Science*, **53**, 7 (2011). Doi: https://doi.org/10.1016/j.corsci.2010.09.046